Journal of Adhesion Science and Technology
December 2010, Volume 24, Numbers 11-12, pp. 1977-1994
http://dx.doi.org/10.1163/016942410X507696

Analysis of the Influence of Hydrostatic Stress on the Behaviour of an Adhesive in a Bonded Assembly

Cognard, J.Y.[1, *]; Créac'hcadec, R.[1]; Maurice, J.[1]; Davies, P.[2]; Peleau, M.[2]; da Silva, L.F.M.[3]

[1] LBMS, ENSIETA/Université de Brest/ENIB, ENSIETA, 2 rue François Verny, 29806 Brest, France
[2] Materials & Structures Group, IFREMER Brest Centre, 29280 Plouzané, France
[3] Departamento de Engenharia Mecânica, Faculdade de Engenharia da Universidade do Porto, Rua Dr Roberto Frias, 4200-465 Porto, Portugal

*: Corresponding author : Cognard J. Y., email address : jean-yves.cognard@ensieta.fr

Abstract

Generally, adhesives are viscoelastic-plastic materials, for which the development of viscosity and plasticity varies depending on the type of adhesive and the stress state. Various models exist to represent the yield surface, or the so-called elastic limit, taking into account the two stress invariants, hydrostatic stress and von Mises equivalent stress. Moreover, to develop precise pressure-dependent constitutive models, it is necessary to have a large experimental database in order to accurately represent the adhesive strains which are strongly dependent on the tensile-shear loading combination. Under quasi-static loadings, for a given strain rate range viscous effects can be neglected, but only a few experimental results are available to model the behaviour of the adhesive in a bonded assembly accurately under realistic loadings. Moreover, edge effects often have a large influence on the mechanical response. This paper presents the possibility of combining the use of an experimental device, which strongly limits the influence of the edge effects, with a pressure vessel especially designed to study the influence of hydrostatic stress. The latter allows pressures up to 100 MPa to be applied during mechanical testing. Comparisons with results obtained with a modified Arcan device are presented. Such results are useful for the development of 3D pressure-dependent models for the yield function and for the analysis of more complex loading.

Keywords: Adhesive testing; non-linear behaviour; modelling; hydrostatic stress; finite element analysis

1. Introduction

Adhesively bonded assemblies are widely used in different industries, and it is a particularly interesting technique for assembling composite structures [1]. But, as the behaviour of an adhesive in an assembly can depend on various parameters (edge effects, type of loading, manufacturing conditions, environment, *etc.*), the analysis of such structures is quite complex. Various models have been proposed [2] but the development of accurate 3D models, which is necessary to analyse and optimize the mechanical behaviour of complex industrial structures, requires a large database of experimental results. Various published studies have indicated an influence of the hydrostatic stress on the behaviour of adhesives, which can be explained by the nature of the adhesive, i.e. a polymer, and by the property of a thin film between thick substrates. Initially, criteria including the hydrostatic stress were proposed as evolutions of the von Mises or Tresca criteria [1]. More significant

evolutions followed, starting from the Drucker-Prager criterion [3]. Various versions of this criterion have been proposed: linear, hyperbolic or Exponential Drucker-Prager (EDP) [3, 4]. The EDP criterion corresponds to that initially developed by Raghava for bulk polymers [5] and has been used to model the behaviour of adhesively bonded joints [6]. However, for adhesives, the usual associated flow rules cannot be used to represent the plastic evolutions accurately [3, 7-10]. A more precise description of the elasto-plastic behaviour of an adhesive can be based on the use of a pressure-dependent constitutive model associated with the definition of a specific yield function and using non-associated formulations introducing another function to describe the flow rules. But very few experimental data are available in order to validate such models.

In previous studies, a large database of experimental results was generated under tensile-shear loadings obtained using a modified Arcan fixture [11]. A non-associated elasto-visco-plastic 2D model, suited to interface-type elements, was proposed to represent the behaviour of an adhesive film in an assembly [12] (epoxy resin Huntsman™ Araldite® 420 A/B). This model can be adapted to solid finite elements using a finite strain formulation. However, the development of 3D models, which are necessary to analyse industrial applications, requires more experimental information in order to accurately represent the yield surface.

In the present study, in order to analyse the influence of the hydrostatic stress on the non-linear behaviour of an adhesive (epoxy resin Huntsman™ Araldite® 420 A/B, cured at 50°C for 4 hours after curing for 12 hours at 20 °C), tests were first performed on bulk adhesive samples in a specially designed pressure vessel, which allows pressures up to 100 MPa to be applied during mechanical testing. Results from these tests are presented first. The second part of the paper shows how the hydrostatic stress affects the mechanical behaviour of the same adhesive in a bonded assembly, using a modified thick adherend shear test (TAST) designed to strongly limit the influence of edge effects. The last part presents, for the same adhesive, the first steps in the development of a 3D pressure-dependent constitutive model. The use of the database of experimental results from tensile-shear tests allows identification of the so-called initial yield function in the hydrostatic stress – von Mises equivalent stress plane. Comparisons between numerical and experimental results underline the possibilities of applying 3D Drucker-Prager type constitutive relations for modelling the behaviour of an adhesive in an assembly.

2. The experimental hydrostatic pressure device (CHEM pressure vessel)

Tests on adhesives and bonded assemblies were performed in the CHEM system [13] (Caisson Hyperbare d'Essais Mécaniques), a pressure vessel especially designed at IFREMER Brest Centre to study the influence of hydrostatic stress on the mechanical behaviour of materials. This pressure vessel allows pressures up to 100 MPa (1000 bars) to be applied during mechanical testing. Figure 1(a) shows the CHEM pressure vessel mounted on a standard tensile testing machine. Up to a pressure of 60 MPa view-glasses can be used to see the inside of the pressure vessel and to allow a non-contact measurement system by image correlation (Fig. 1(b)). Above this pressure, metallic closures have to be used instead of the view-glasses. After positioning the specimen in the tensile testing machine, the vessel is closed using the screw-nut system presented in Fig. 1(b). The vessel is then filled with tap water and the required pressure is applied, using a special pump. It is important to note that while the pressure is increasing, a specific two-chamber equilibrium system ensures no preloading of the specimen. A mechanical test can then be performed under a given pressure in the vessel; the mechanical loading being imposed by the tensile testing machine. Other experiments have been performed previously in this vessel and point out the reliability for this experimental device [13,14].

Unless noted otherwise, all the tests presented below were performed by controlling the displacement of the crosshead of the tensile testing machine at 1 mm/minute.

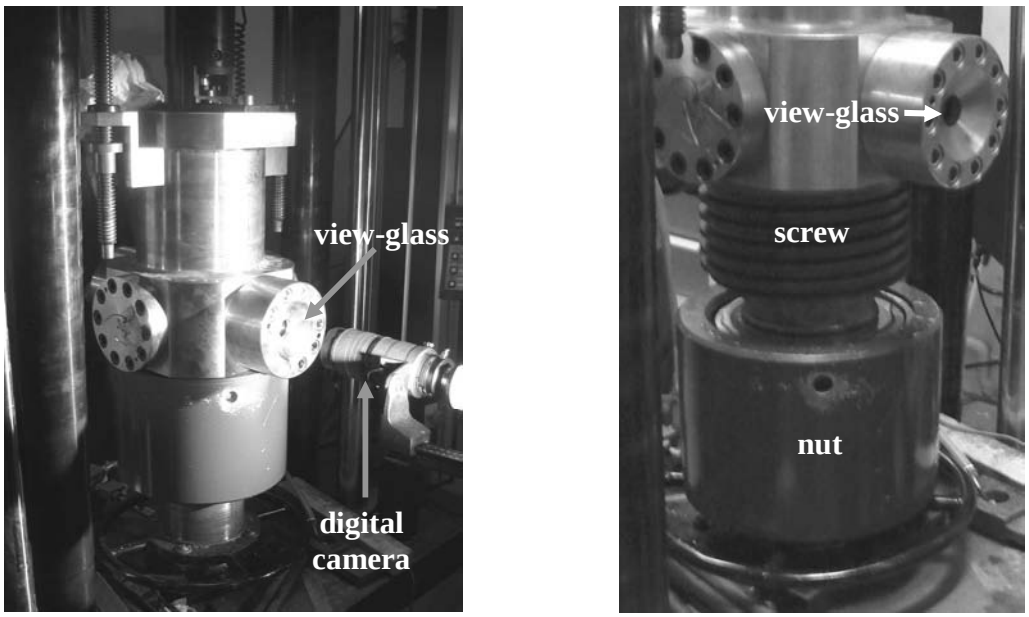

(a) (b)

Figure 1. Presentation of the CHEM system, a pressure vessel especially designed to study the influence of hydrostatic stress on the mechanical behaviour. (a) The CHEM system with the use of a digital camera and (b) the closing system (screw-nut) of the pressure vessel.

3. Experimental results for bulk adhesive

Figure 2b presents, in the form of load-time diagrams, some results for bulk specimens, cast directly with a dogbone geometry having a central section of 4 mm x 10 mm. The technique described in the French standard NF T 76-142 [15] for producing plate specimens without porosity was used [16]. Figure 2(a) presents a bulk specimen at failure, after opening of the pressure vessel. Figure 2(b) shows how the load varies with time for different pressures in the pressure vessel. In order to be able to compare the results directly, all the tests were performed in the CHEM pressure vessel. A pressure of 0.5 MPa corresponds to the very low hydrostatic stress loading of a specimen simply immersed in water as for the other tests. It can be noted that an increase of the hydrostatic stress loading leads to an increase in the failure load for these specimens. Figure 3 shows the so-called elastic limit for a given displacement rate of the tensile testing machine crosshead (V = 1 mm/min) in the hydrostatic stress - von Mises equivalent stress diagram, for different values of the hydrostatic stress loading in the vessel. The loading paths for bulk adhesive tests, under elastic behaviour, in the CHEM pressure vessel are presented in the same diagram.

The CHEM pressure vessel allows quite complex loading paths for the adhesive, and the results underline the influence of hydrostatic stress on the adhesive behaviour. During the closure of the CHEM system, some parasitic loads on the specimens were observed due to small transverse displacements, which may have a slight influence on the measured results. Also, as the adhesive studied shows appreciable viscous behaviour, such tests are characterized with a lower strain rate than similar experiments on an adhesive in a bonded assembly. Moreover, such tests do not take into account the presence of the interfaces between the adhesive and the substrates which exist in bonded assemblies. Comparison of

results from bulk tests with those for adhesive in a bonded assemblies is always a delicate exercise.
In order to avoid these difficulties, the next section presents results from shear tests on the adhesive in a bonded assembly, using a specific fixing system to the tensile testing machine in order to prevent parasitic loads during the different phases of the test.

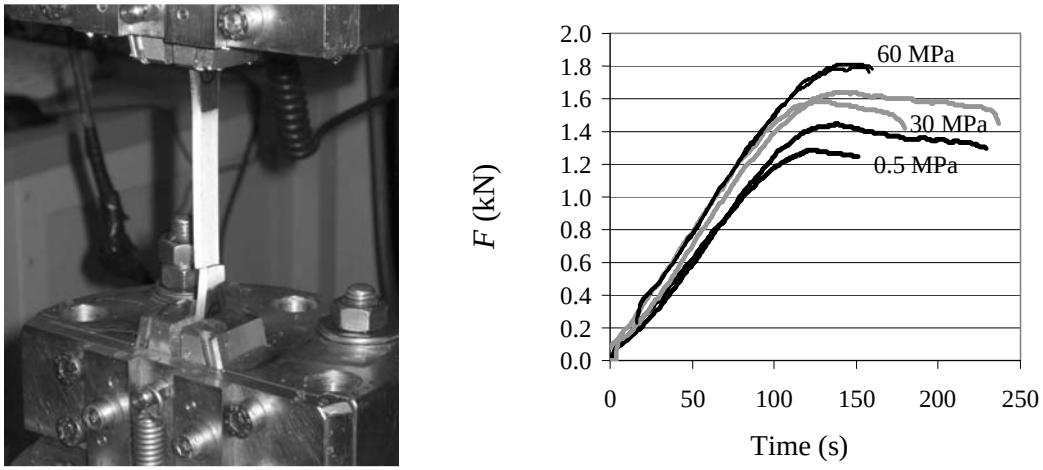

(a) (b)

Figure 2. Experimental results with bulk specimens for different hydrostatic stresses and for a given displacement rate of the tensile machine crosshead (V = 1 mm/min). (a) Bulk specimen at failure and (b) experimental results in the load-time diagram (two curves for each pressure).

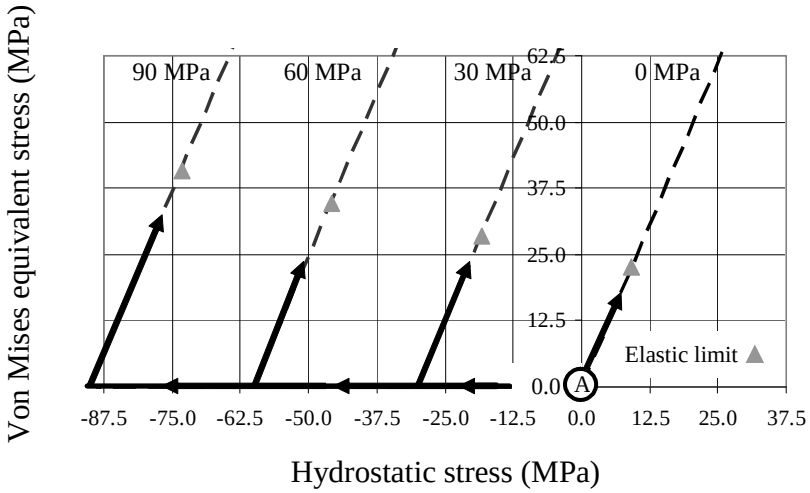

Figure 3. Experimental elastic limits for bulk tests, for a displacement rate of the tensile machine crosshead V = 1 mm/min and for 4 loading paths at different pressures (0, 30, 60 and 90 MPa); the dashed lines represent, under elastic behaviour, the loading path in the CHEM system.

4. Experimental results from shear tests on adhesive bonded assembly

4.1. The modified TAST fixture

The thick adherend shear test (TAST) can be seen as an optimized single lap shear test. It is widely used to evaluate adhesive systems [17-18]. The test is detailed in an ASTM standard and with a suitable extensometer it allows to obtain a full shear stress-shear strain curve to

[19]. It has been shown that for such tests, cracks can appear quickly at the two edges of the adhesive joint close to the adhesive-substrate interfaces [20]. In order to improve the TAST fixture, the first step was to use small bonded samples (Fig. 4) which represent the useful part of the TAST specimen (a parallelepiped of height approximately 20 mm with an adhesive section of *Sc* = 9.53 mm x 25.4 mm) [21]. A simple preparation of aluminium bonded surfaces was used (abrasion with 120 grade paper and acetone degreasing). The modified TAST fixture, presented in Figs 4(a) and 4(b), uses a support (2) and a fastening device (3). The supports (Figs 4(a) and 4(b) are very rigid in order to limit the influence of edge effects [11]. Specific mechanical joints [22] were used to connect the modified TAST fixture to the tensile testing machine, in order to prevent parasitic loads during the different phases of the test.

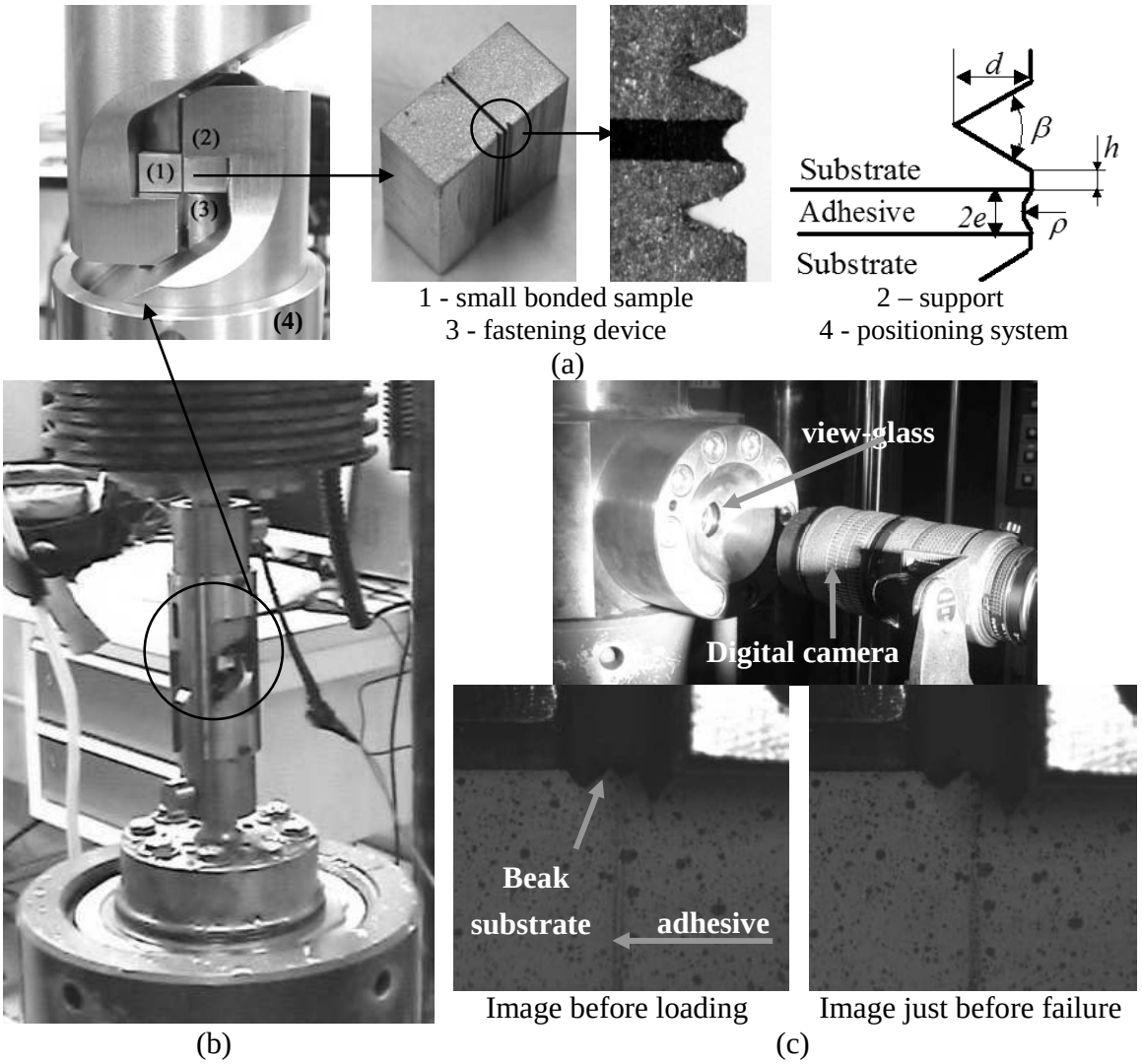

Figure 4. The modified TAST fixture in the CHEM pressure vessel. (a) Geometry of the bonded specimen, (b) the modified TAST fixture and (c) the measurement of the adhesive deformation with an image before loading and an image just before failure.

The measurement of strain through the view-glass, with a digital camera and image analysis system already used in a previous work [11] (Fig. 4(c)), enabled the influence of the pressure loading (up to 60 MPa) to be studied and analysed during the tensile tests. It is important to note that the displacement measurements in the CHEM pressure vessel,

through the view-glass, with a digital camera is a difficult task, and requires great care with calibration and lighting. Figure 4(c) presents the images at the initial moment (point *A* in Fig. 3) and just before failure.
In the following, the term *DT* denotes the relative displacements of both ends of the adhesive in the tangential direction. *DT* was obtained with a non-contact measurement system based on image correlation. *FT* represents the tangential component of the applied load in the tangential direction in the mean plane of the adhesive (the normal component is equal to zero for shear loading).

4.2. Experimental results

Figure 5 presents results for four hydrostatic stress loads (0.5, 30, 60, 90 MPa). Figure 5(a) shows the load versus time plots and indicates the influence of the hydrostatic stress on the behaviour of the adhesive in a bonded assembly under shear loadings.

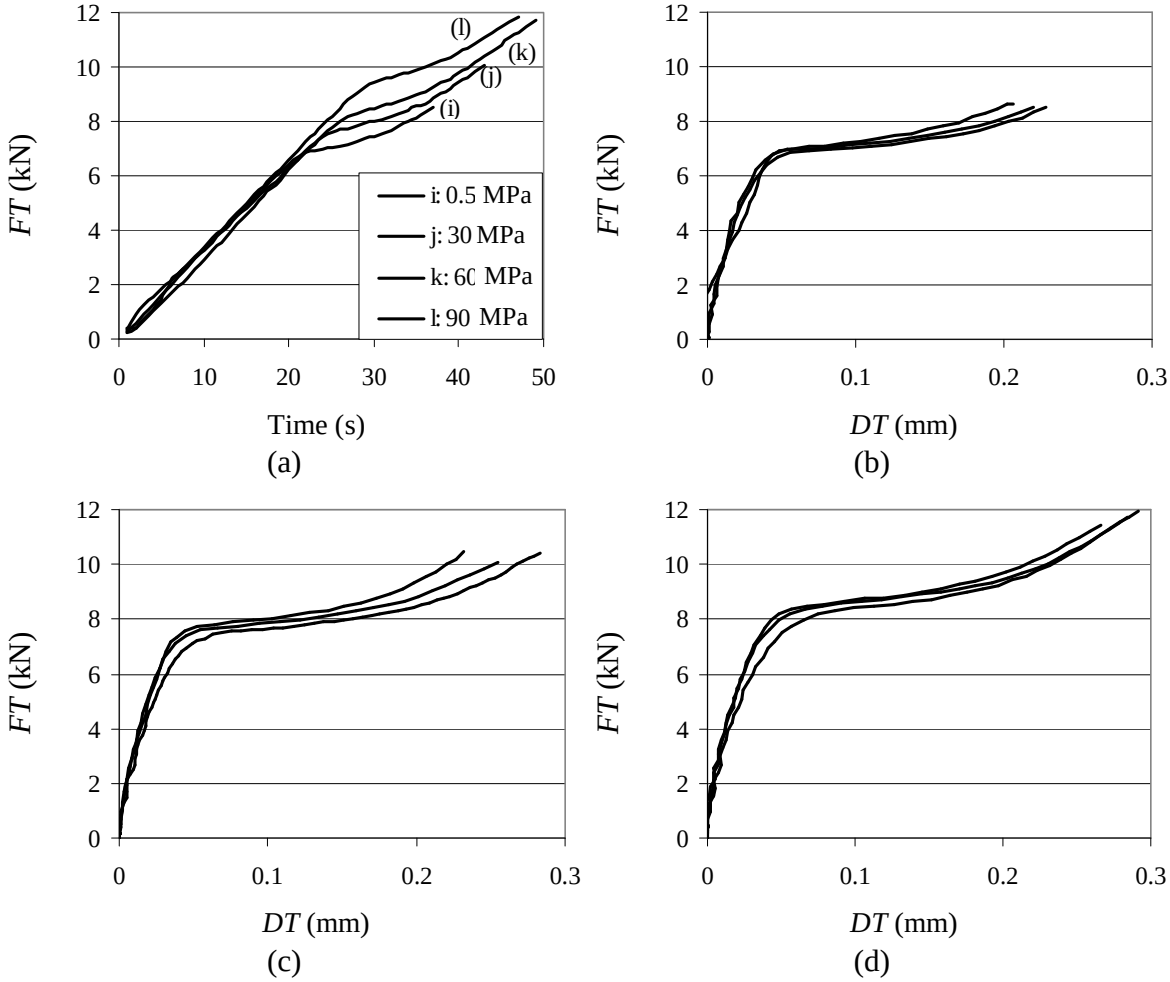

Figure 5. Experimental results with the modified TAST device for different pressures, for a bondline thickness of 0.2 mm and for a crosshead displacement rate V = 1 mm/min. (a) Load-time diagram, (b) load-displacement diagram for a pressure p = 0.5 MPa, (c) load-displacement diagram for a pressure p = 30 MPa and (d) load-displacement diagram for a pressure p = 60 MPa.

An idea of the scatter in the experimental results is presented in Figs 5(b), 5(c) and (d) in the load-displacement diagrams. These figures give results from tests on three specimens

and indicate that the variability is quite low for such tests. The measurement technique used does not allow us to analyse the deformation of the adhesive during the increase of the hydrostatic pressure loading. In order to analyse the effect of the first part of the loading, which can also be influenced by viscous effects, numerical simulations can be done in order to precisely analyse the real behaviour of this experimental test, but they require 3D simulations.

4.3. Three-dimensional analyses

To determine the stress state in the adhesive during the different phases of the loading path, 3D models were used, with the assumption of elastic behaviour for both the adhesive and the adherends. In this study, the support was not modelled in order to limit the model size. In addition, the calculation was performed on one quarter of the specimen, using appropriate boundary conditions (shown in Fig. 6(b)). The model contains 756,314 nodes (2,268,942 degrees of freedom) and 840,412 linear elements. The adhesive is meshed with solid elements with 401,842 nodes (1,205,526 degrees of freedom). For these computations, aluminium substrates were used (Young modulus: E_S = 75 GPa, Poisson's ratio: ν_S = 0.3) and the elastic parameters of the adhesive were chosen as: E_a = 2 GPa, ν_a = 0.40 (identified previously [12]). The numerical finite element simulations presented in this section were performed with the CAST3M code (CEA, Saclay, France) [21]. The mechanical loading (Fig. 6(b)) is a nominal displacement in the x direction.

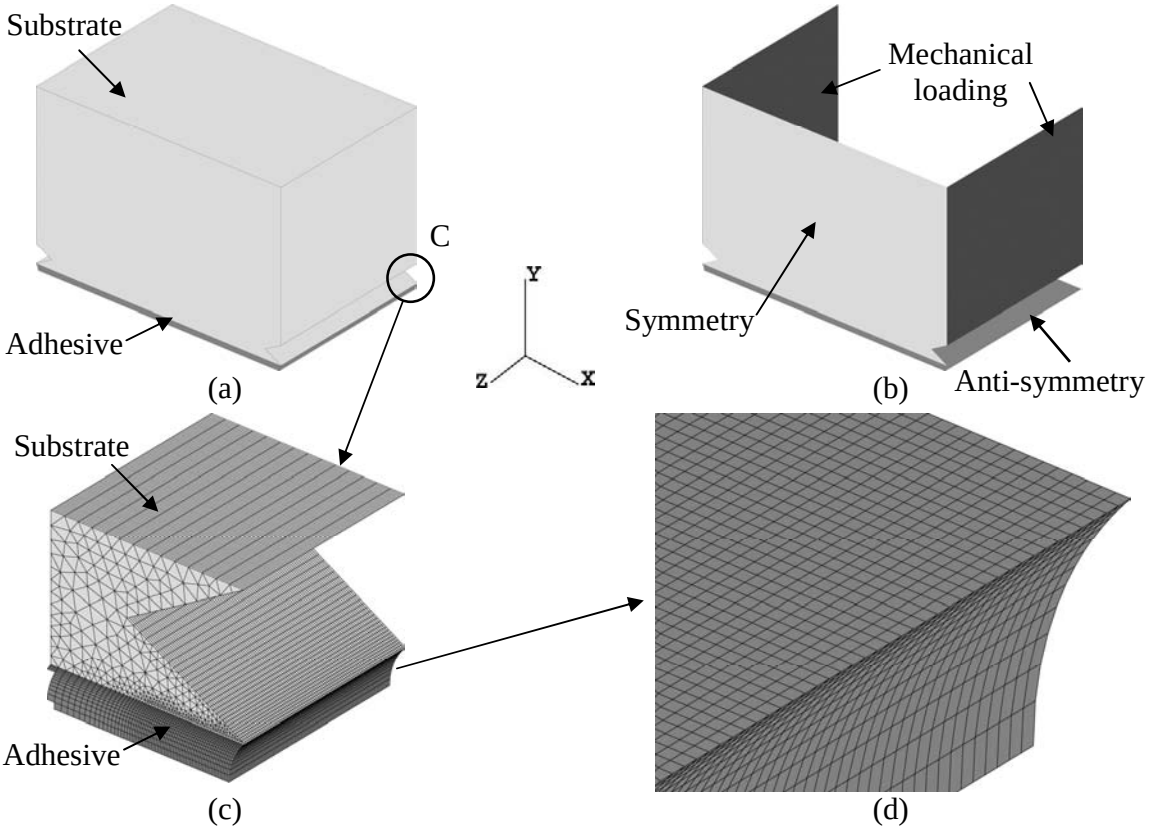

Figure 6. Model used for the 3D calculation of the modified TAST specimen. (a) Model with beaks, (b) boundary conditions, mesh of beak and (d) mesh of the adhesive (close-up view).

Figure 7 presents the three dimensional distributions of the von Mises equivalent stress and of the hydrostatic stress in the half-adhesive layer for the modified TAST specimen under a

hydrostatic stress loading. For a given plane in the adhesive (i.e. for a given y, y = 0 corresponds to the mid-plane of the adhesive layer), the von Mises equivalent stress and the hydrostatic stress are represented on the y-axis. For these graphs, as the computation was done under elastic assumption, the maximal value of the equivalent von Mises stress in the adhesive was normalized to 1., in order to simplify the presentation. It is important to note that the von Mises equivalent stress is nearly constant through the bondline thickness (Figs 7(a) and 7(c)), which underlines the low influence of the edge effects due to the use of sharp beaks and cleaning of the free edges of the adhesive [22]. The middle of the joint is loaded under pure shear and thus the hydrostatic stress is equal to zero (Fig. 7(b)). Close to the beaks and close to the adhesive – substrate interface a low level of hydrostatic stress can be noted (Fig. 7(d)).

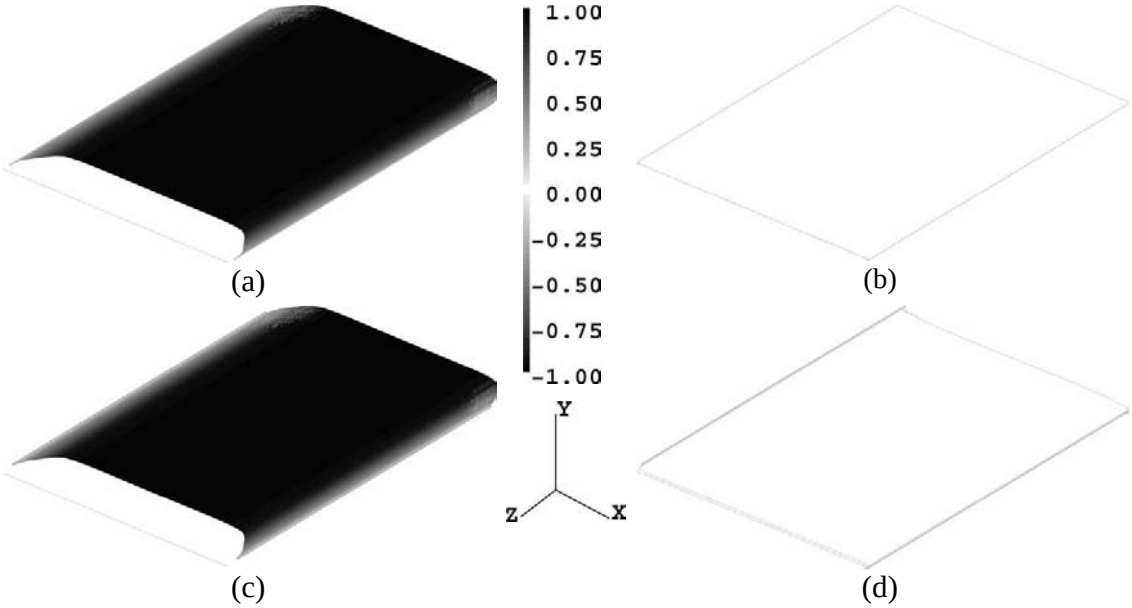

Figure 7. Evolution of the von Mises equivalent stress and the hydrostatic stress in the adhesive for the modified TAST specimen under a shear loading (elastic assumption) for different positions in the adhesive (y = 0 represents the mean plane of the adhesive and $y = e$ is close to the adhesive-substrate interface (2e denote the bondline thickness). (a) Von Mises equivalent stress for y = 0, (b) hydrostatic stress for y = 0, (c) von Mises equivalent stress for $y = e$ and (d) hydrostatic stress for $y = e$.

Figure 8 presents the space evolution of the von Mises equivalent stress and of the hydrostatic stress in the half-adhesive for the modified TAST specimen under a hydrostatic stress loading using the same layout as for Fig. 7. The results show that the stress state in the adhesive is quite complex. The central part of the adhesive (z = 0) is nearly loaded in compression in the y direction (Fig. 8) associated with the pressure. The hydrostatic stress loading applied in the periphery of the joint affects only a small region of the adhesive close to the edge. Close to the free edge of the adhesive in the z direction (Fig. 8) an increase of the von Mises equivalent stress can be noted. In fact, for this edge the specimen manufacturing process used results in a straight edge of the adhesive, there is no beak. Such a geometry does not lead to stress concentrations under shear loading (Fig. 7) but hydrostatic stress loading leads to some edge effects. This stress concentration does not seem to affect the behaviour of the test strongly, as no crack initiations were observed here, and during the loading path the transmitted load is increased continuously until failure, which was obtained for a quite large adhesive strain ($DTmax \approx 0.25$ mm for a bondline thickness of $2e$ = 0.2 mm, Fig. 5). Large stress concentrations in bonded specimens can

cause crack initiation at quite low adhesive strain [20]. Nevertheless, for tests under hydrostatic stress loadings, the geometry of the bonded specimen used in the modified test could be optimised in order to limit the influence of edge effects, by machining beaks all around the substrates [20], but the machining process has to be adapted [22].

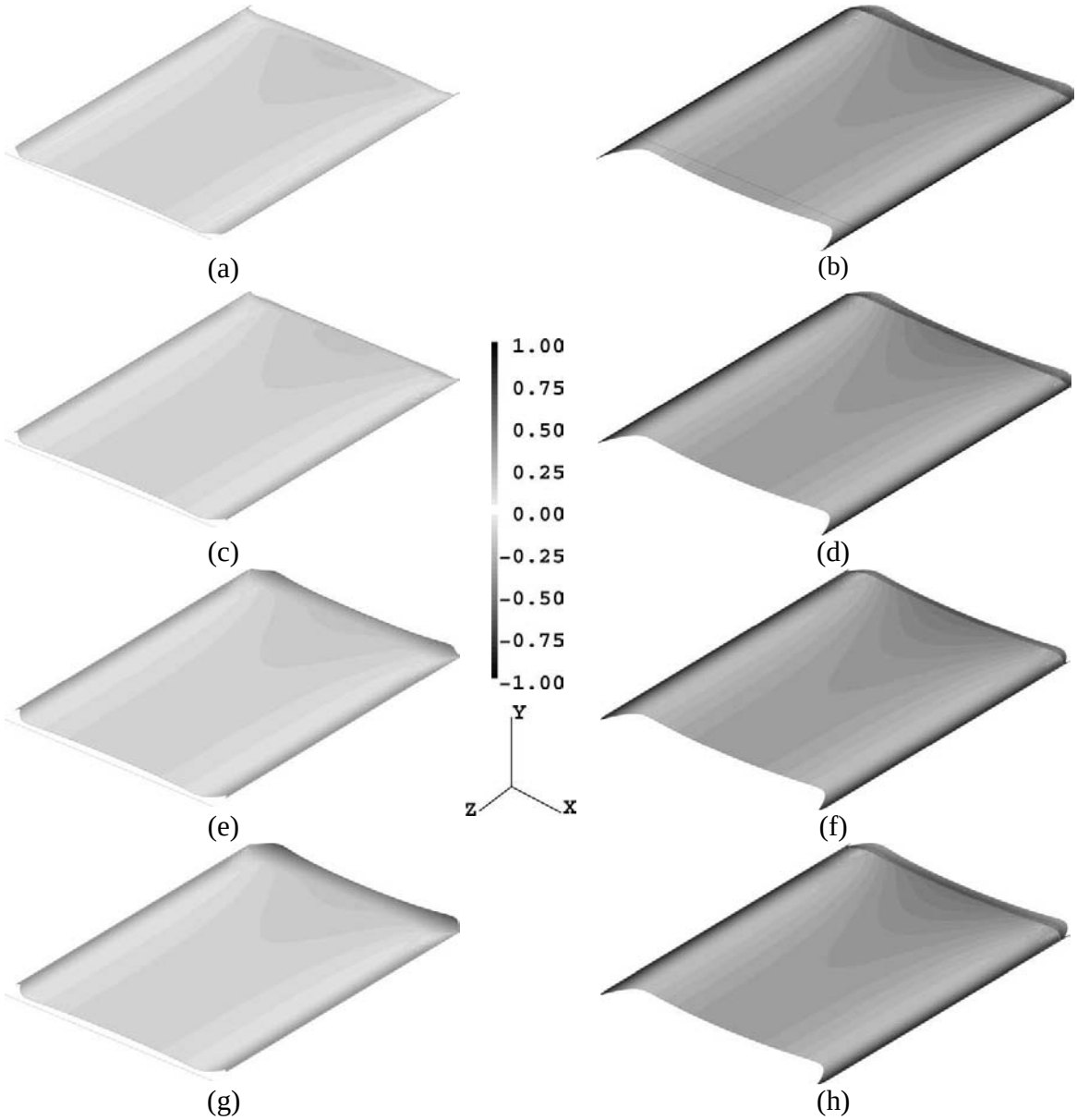

Figure 8. Evolution of the von Mises equivalent stress and the hydrostatic stress in the adhesive for the modified TAST specimen under a hydrostatic stress loading (elastic assumption). (a) Von Mises equivalent stress for $y = 0$, (b) hydrostatic stress for $y = 0$, (c) von Mises equivalent stress for $y = e/2$, (d) hydrostatic stress for $y = e/2$, (e) von Mises equivalent stress for $y = 3e/4$, (f) hydrostatic stress for $y = 3e/4$, (g) von Mises equivalent stress for $y = e$ and (h) hydrostatic stress for $y = e$.

The results allow the determination of an approximate elastic limit and the loading path in the central part of the joint for the proposed test under elastic assumption, for the different imposed hydrostatic stress loadings (Fig. 9). To a first approximation, a constant shear stress is assumed.

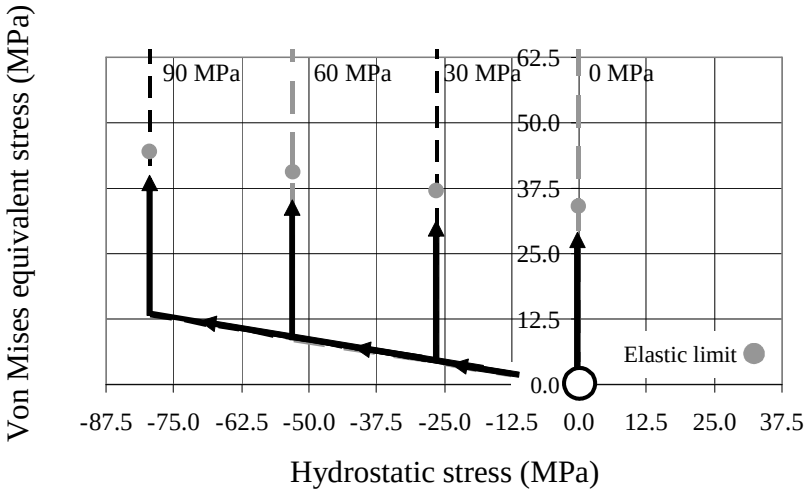

Figure 9. Experimental elastic limits for modified TAST specimens with a bondline thickness of 0.2 mm, for a displacement rate of the tensile machine crosshead V=1mm/min and for 4 loading paths at different pressures (0, 30, 60 and 90 MPa); the dashed lines represent, under elastic behaviour, the average loading path in the CHEM system.

5. Development of a pressure-dependent constitutive model

5.1. Results of modified Arcan tests

In order to develop an accurate model of the non-linear behaviour of the adhesive in a bonded assembly, an experimental study of the influence of the peel stress has been performed with a modified Arcan fixture [23], which enables compression or tension to be combined with shear loads [11]. The design of this modified Arcan fixture has been described previously (use of beaks, cleaning of the free edges of the adhesive, fixing system of the bonded specimen) and it allows the edge effects to be significantly reduced, and pre-loading of the adhesive to be avoided (Fig. 10) [11]. For this test, a bonded specimen with rectangular section (10 mm x 65 mm) was tested. The main parameters which define the geometry of the bonded specimen are: e = 0.2 mm, h = 0.2 mm, d = 0.5 mm, r_0 = 0.25 mm, ρ=1.5 e, α=45° (Fig. 10(c)). A non-contact extensometry system based on image correlation, allows us to analyse the deformation of the adhesive joint [11]. In the case of linear elastic behaviour, the stress distribution is not constant in the adhesive for the modified Arcan test, thus inverse identification techniques have to be used in order to analyse the experimental results [12].

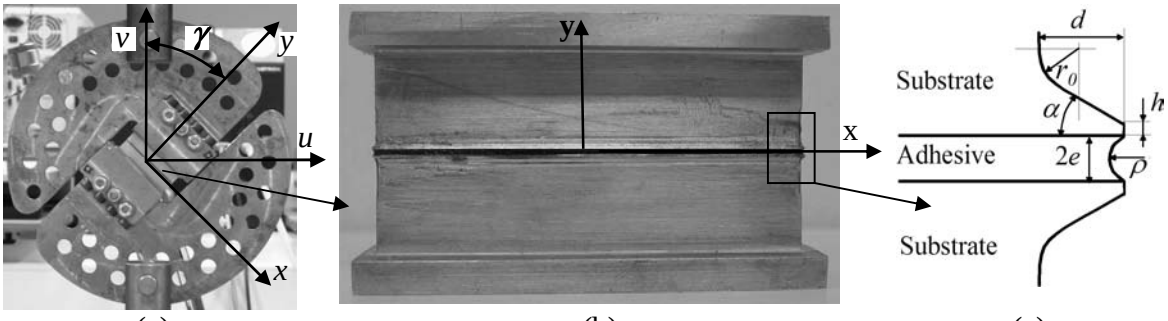

Figure 10. The modified Arcan fixture. (a) Tensile-shear test, (b) geometry of the bonded specimens and (c) geometry of the beak.

DN and *DT* denote the relative displacements of both adhesive-substrate interfaces, respectively in the normal and tangential directions of the mean plane of the adhesive (respectively, direction *y* and *x* defined in Fig. 10(b)). *FN* and *FT* represent the components of the applied load in the normal and tangential directions.
The experimental and 3D numerical results were used in order to estimate the yield function in the hydrostatic stress – von Mises equivalent stress diagram (Fig. 11). Moreover Fig. 11 presents the average loading paths, under elastic behaviour, for the different tests associated with the angle γ defined in Fig. 10(a).

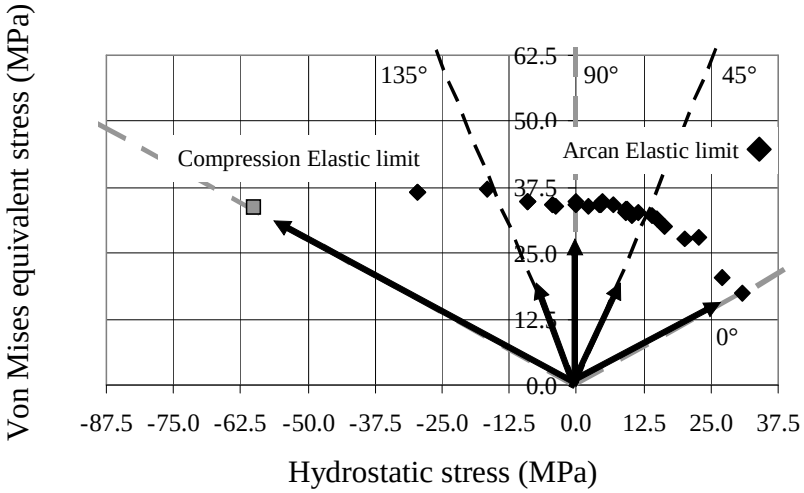

Figure 11. Experimental elastic limit for a displacement rate of the tensile machine crosshead V = 0.5 mm/min, for a bondline thickness of 0.4 mm and average loading path, under elastic behaviour, for modified Arcan tests with respect the angle γ (see Figure 10a) and for a compression test (dashed lines).

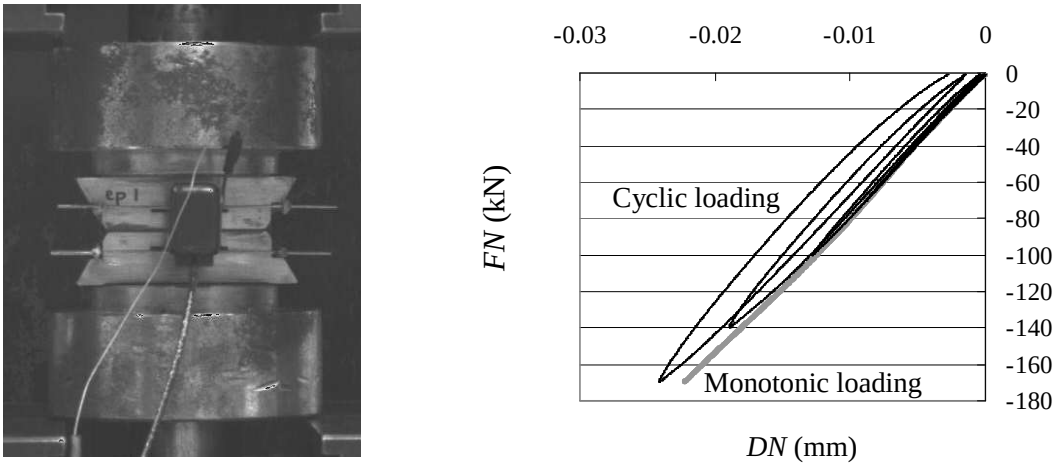

Figure 12. Results of compression tests for an adhesive in a bonded assembly. (a) Compression test used and (b) behaviour in the normal direction.

The proposed Arcan fixture does not allow to apply compression (γ = 180°) due to design constraints. Thus, some additional tests were performed, by placing a bonded specimen between two plates and using a classical extensometer, as the level of deformation of the adhesive under compression is quite low (Fig. 12). For such tests, the determination of the

elastic limit of the material is difficult. Moreover, the influence of parasitic positioning is difficult to analyse. This test should be optimised in order to obtain more precise results.

5.2. Identification of the initial yield function

Starting from the experimental results obtained with the modified TAST specimen in the CHEM system (adhesive thickness of 0.2 mm and displacement rate of the tensile testing machine crosshead of 1 mm/min) and the results obtained with the modified Arcan device (adhesive thickness of 0.4 mm and displacement rate of the tensile testing machine crosshead of 0.5 mm/min) it is possible to define the initial yield function for the adhesive (neglecting the viscous effects), Fig. 13. Experimental results for bulk specimens are also presented in Fig. 13 for comparison. They are not used to identify the yield surface because it has been emphasized previously that the experimental conditions are not the same as for the tests on an adhesive in a bonded assembly.

An Exponential Drucker-Prager yield function ($F_0 = 0$) allows a good representation of the experimental data for the initial so-called elastic limit:

$$F_0 = a\,(\sigma_{vm})^{b} + p_h - p_{t0} = 0 \qquad (1)$$

Where σ_{vm} is the von Mises equivalent stress and p_h is the hydrostatic stress. a, b and p_{t0} are material parameters. The results of the identification are presented in Table 1 and the initial yield surface is drawn in Fig. 13.

Table 1. Material parameters for the initial yield surface (defined by the equation (1)).

a (SI units)	b	p_{t0} (MPa)
1. E-6	4.87	31.7

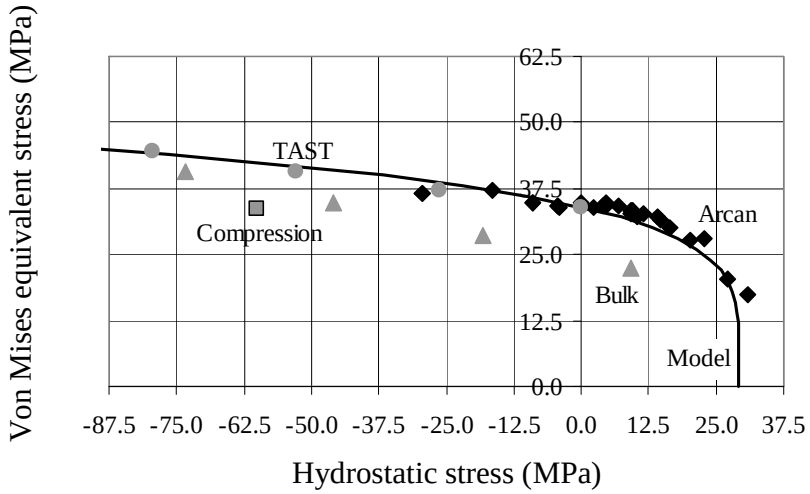

Figure 13. Presentation of the so-called elastic limit in the von Mises equivalent stress - hydrostatic stress diagram for different tensile-shear tests and the proposed identified yield function.

5.3. Possibilities of Drucker-Prager type models

The development of a 3D model has to take into account the various experimental observations. It is important to note that for the adhesive studied, at failure under shear the relative displacement of both ends of the joint is nearly equal to the adhesive thickness; therefore, finite element simulations have to be carried out under the assumption of finite transformations. Moreover, the deformation of the adhesive in the direction normal to the

midplane of the joint is lower than in the tangential direction (a factor of 10 or more can be noted) [11].
Some simulations have been performed using the Exponential Drucker-Prager non associated model implemented in the finite element code Abaqus [24] in order to analyse the possibilities of such model for this problem. The elastic parameters of the adhesive were chosen as: E_a = 2 GPa, ν_a = 0.40 (identified from previous analysis [12]). The evolution of the yield surface is described as follows:

$$F = a\,(\sigma_{vm})^{b} + p_h - p_t \tag{2}$$

Where p_t is the hardening parameter. The evolution of the function p_t is such that:

$$p_t = a\,(\sigma_t)^{b} + \frac{\sigma_t}{3} \tag{3}$$

σ_t is obtained from the plastic behaviour under pure tensile loading (Fig. 14).
The flow rules are obtained from the following flow rule function:

$$G = \left((\delta\,\sigma_{t0}\tan(\psi))^{2} + (\sigma_{vm})^{2} \right)^{1/2} + p_h \tan(\psi) \tag{4}$$

where σ_{t0} is the initial elastic limit in traction, ψ is the dilation angle and δ is a material parameter.

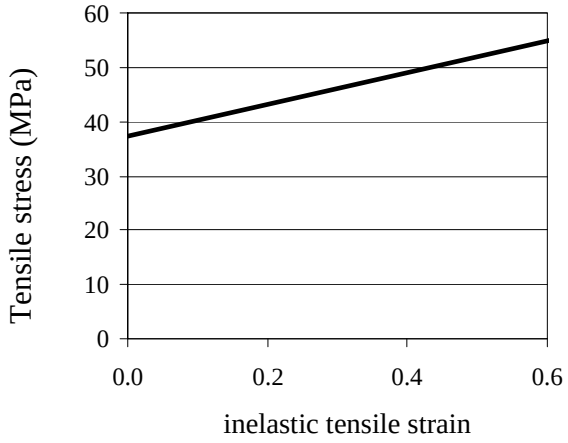

Figure 14. Behaviour of the adhesive in the stress-inelastic strain under pure tensile loading used for the computations.

Finite element analyses were performed with Abaqus 6.6 [24] considering a simplified geometry of half the specimen. Beaks were not considered and only one layer of elements was used to mesh the adhesive joint (Fig. 15). In a first approach, these two simplifications allow the calculation time to be reduced by maintaining a state of stress similar to the one obtained with a fine mesh. The model contains 50,430 8-node linear bricks elements. The support was not considered and appropriate boundary conditions were applied.
The results from a first optimisation of the proposed model parameters, starting from some usual values [4, 6] in order to represent tensile-shear loadings for an adhesive in an assembly are presented in Table 2 and in Fig. 14.
Computations have been made for the modified Arcan test using 3D model under shear loading (γ= 90°) and under tensile-shear loading (γ= 30°) using aluminium substrates. For these two loadings, the load-displacement curves obtained by applying the proposed model in the computational analyses are in good agreement with the experimental ones (Figs 16 and 17). The model parameters have been mainly identified starting from the shear test

(Fig. 16). For a tensile-shear loading defined with $\gamma = 30°$, the results presented in Fig. 17 underline that non-associated Exponential Drucker-Parger type models are able to represent the large ratio between the inelastic displacements in the normal and tangential directions. An optimisation of parameters of the model (evolution of the hardening, definition of the flow rule function, *etc*) is necessary in order to accurately represent the behaviour under compression - shear loadings.

Table 2. Material parameters for the flow rule of the non-associated Drucker-Parger type model (defined by the equation (2)).

σ_{t0} (MPa)	δ	$\psi(°)$
37.24	0.1	25°

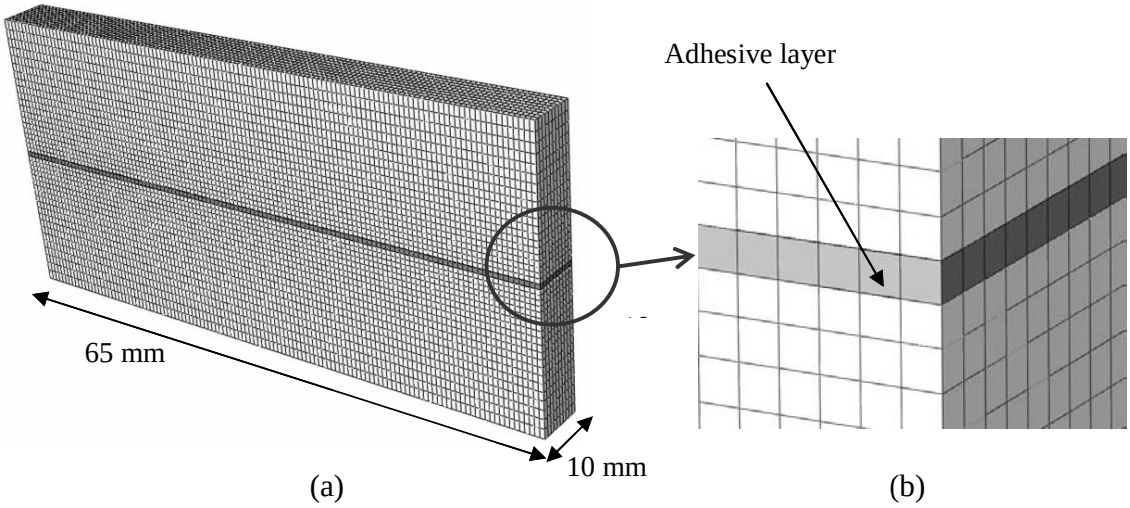

Figure 15. Simplified finite element model for the Arcan specimen. (a) Model and mesh with no beaks and (b) mesh at the ends of the joint.

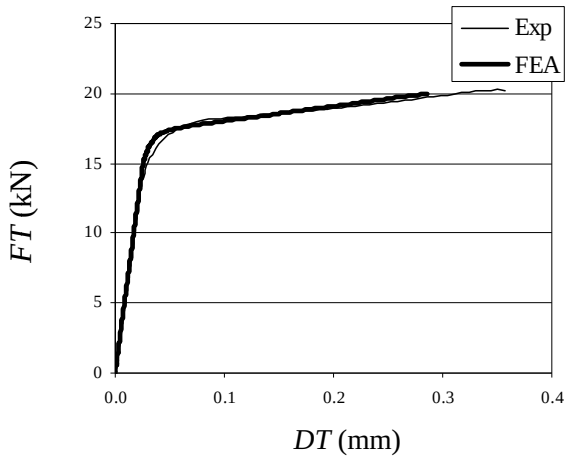

Figure 16. Comparison, in the tangential direction, between experimental ('Exp' in graph) and finite element analysis ('FEA' in graph) Arcan results for shear loadings ($\gamma = 90°$, in Fig. 10).

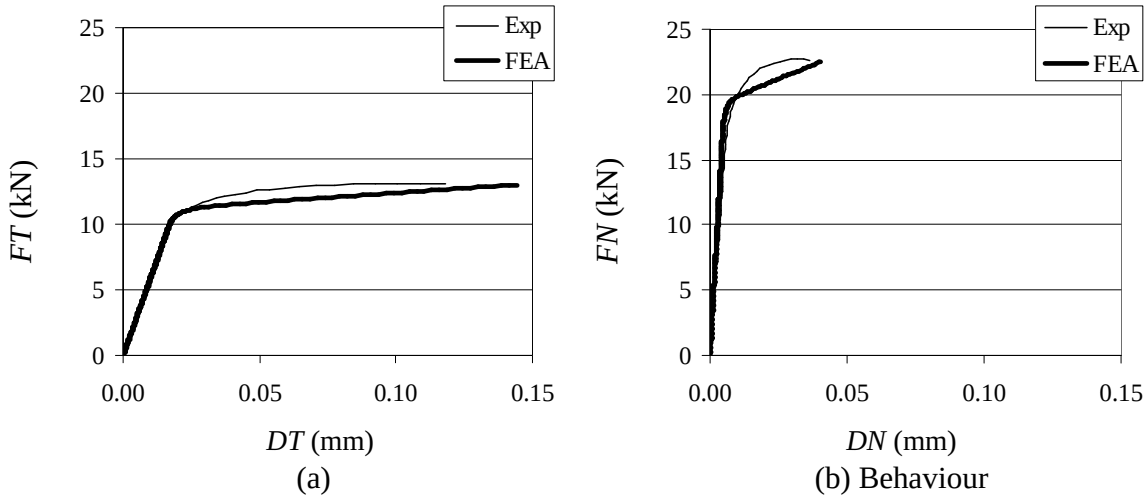

(a) (b) Behaviour

Figure 17. Comparison between experimental ('Exp' in graph) and finite element analysis ('FEA' in graph) Arcan results for tensile-shear loadings (γ = 30°°, in Fig. 10). (a) Behaviour in the tangential direction, (b) behaviour in the normal direction.

6. Conclusions

The behaviour of an adhesive in a bonded assembly is quite complex to model. Various pressure-dependent constitutive models exist in the literature; but in any case, a large experimental database is necessary in order to accurately represent the adhesive behaviour. In a previous study, the influence of tension/compression-shear loadings was analysed using a modified Arcan type fixture. To complete this database, new results have been obtained using a specific shear test (so-called modified TAST) in a pressure vessel especially designed to study the influence of hydrostatic stress up to 100 MPa on the mechanical behaviour. It has been shown for shear tests that an increase of the hydrostatic stress leads to an increase of the so-called elastic limit as well as of the failure load. These results allow an accurate identification of the initial yield function of the adhesive for a given strain rate, taking into account the two stress invariants, hydrostatic stress and von Mises equivalent. Moreover, the different experimental tests proposed provide the global response of the adhesive in the bonded assembly in the form of a load – displacement diagram. Thus, these experimental results are useful to accurately identify the non-linear constitutive model of the adhesive. The first results obtained are encouraging.

This study has to be continued in order to analyse experimentally and numerically more complex loadings. On the one hand, cyclic loadings using the modified TAST specimens in the CHEM pressure vessel, and on the other, by applying other loading paths by placing a modified Arcan device inside the CHEM system. The bonded specimens which will be used with the modified Arcan device should be manufactured with beaks all around the substrates, in order to limit the influence of edge effects for the different loading paths.

Acknowledgements

The authors wish to acknowledge METRI-2 European project for financial support. The authors are grateful to Bernard Leilde and Albert Deuff from IFREMER for their collaboration in the experimental tests with the CHEM system. We also thank particularly Hervé Trébaol, Pierre Martinat and Bruno Mecucci from ENSIETA/DTN/CMA for their collaboration in designing and manufacturing the modified TAST fixture.

References

[1] R.D. Adams (Ed.), Adhesive Bonding: Science, Technology and Applications, Woodhead Publishing Limited, England (2005).
[2] L.F.M. da Silva and A. Öchsner (Eds.), Modeling of Adhesive Bonded Joints, Springer, Berlin (2008).
[3] C. H. Wang and P. Chalkley, Int. J. Adhesion Adhesives **20**, 155-164 (2000).
[4] G. Dean, L. Crocker, B. Read and L. Wright, Int. J. Adhesion Adhesives **24**, 295-306 (2004).
[5] R.S. Raghava and R. M. Cadell, J. Mater. Sci. **8**, 225-232 (1973).
[6] A. Deb, I. Malvade, P. Biswas and J. Schroeder, Int. J. Adhesion Adhesives **28**, 1-15 (2008).
[7] R. Mahnken, Computer Methods in Applied Mechanical Engineering **194**, 4097-4114 (2005).
[8] R. Mahnken and M. Schlimmer, Int. J. Numerical Methods in Engineering **63**, 1461-1477 (2005).
[9] R. Rolfres, M. Volger, G. Ernst and C. Hühne, Trends in Computational Structures Technology, Saxe-Coburg Publications, Stirlingshire, Scoltland, ISBN 978-1-874672-35-7, Chapter 7, pp. 151-171 (2008).
[10] P. Jousset, S. Koch and M. Rachik, Proceedings Euradh'08, Oxford, UK (2008).
[11] J.Y. Cognard, P. Davies, L. Sohier and R. Créac'hcadec, Composite Structures **76**, 34-46 (2006).
[12] R. Créac'hcadec and J.Y. Cognard, J. Adhesion **85**, 239-260 (2009).
[13] P. Davies, D. Cartié, M. Peleau and I.K. Partridge, Proceedings ISOPE (International Symposium on Offshore and Polar Engineering) 2004, Toulon, France (2004).
[14] D. Cartié, P. Davies, M. Peleau and I. K. Partridge, Composites: Part B **37**, 292–300 (2006).
[15] French standard, NF T 76-142 (1988).
[16] L.F.M. da Silva and R.D. Adams, J. Adhesion Sci. Technol. **19**, 109-141 (2005).
[17] W.K. Chiu, P.D. Chalkley, and R. Jones, Computers & Structures **53**, 483-89 (1994).
[18] M. Zgoul, and A.D. Crocombe, Int. J. Adhesion Adhesives **24**, 355-366 (2004).
[19] ASTM D5656-95 (1995).
[20] J. Y. Cognard, R. Créac'hcadec, L. Sohier and P. Davies, Int. J. Adhesion Adhesives **28**, 393-404 (2008).
[21] Cast3m documentation, www-cast3m.cea.fr/cast3m.
[22] J. Y. Cognard and R. Creac'hcadec, J. Adhesion Sci. Technol. **23**, 1333-1355 (2009).
[23] L. Arcan, M. Arcan, and I. Daniel, ASTM Tech Publ **948**, 41-67 (1987).
[24] Abaqus documentation, Version 6.6. Simulia, (2007).